Journal of Engineering Sciences, Assiut University, Vol. 36, No. 1, pp. 1-18, January 2008

NUMERICAL AND EXPERIMENTAL ANALYSIS OF DIVIDING FLOW IN SHORT OPEN CHANNEL TRIBUTARIES

Ali, N.A.,
Prof. of Hydraulics, Civil Eng. Dept., Assiut University, Assiut, 71516 Egypt
Gamal Abozeid,
Associate Prof., Civil Eng. Dept., Assiut University, Assiut, 71516 Egypt
Kamal A.M., and
Lecturer, Civil Eng. Dept., Aswan University, Egypt
Khaled M.A.
Ass. Lect., Civil Eng. Dept., Aswan University, Egypt

(Received March 10, 2007 Accepted September 3, 2007)

Dividing flow in open channel junction is of interest in environmental and hydraulic engineering. It occurs in many hydraulic structures ranging from wastewater treatment facilities to fish passage conveyance structures, irrigation and drainage canals and natural river system. In this research, Schwarz-Christoffel transformation and principle of energy are used to predict the flow rates, the flow depths and values of Froude number in the tributary channels of rectangular open channel junction with three tributary channels. Also, an experimental program is performed to verify the numerical results of the theoretical solutions. The difficulty of a theoretical study of the dividing flow in an open channel due to the flow separation, recirculation regions and possibility of formation of hydraulic jump makes the complete numerical analysis of the problem impossible. However, in this study, with some particular assumptions to the problem, by adopting the conformal mapping technique (Schwarz – Christoffel transformation theory) and by applying the principle of conservation of energy, the flow pattern at a rectangular junction with three tributary channels is simulated; the numerical model is programmed on the computer with MATLAB Version 6.0.0.88 and the flow characteristics are evaluated. The verification of the results of the numerical model shows a will agreement between these results and those from the experimental model. The results revealed that: 1) Froude number in the main channel has negligible influence on the flow rates in the branches. 2) Flow characteristics in the main channel extension or in the branches depend largely on the geometrical dimensions of the junction. 3) The relative depths in the tributary channels independent of the junction geometry.

KEYWORDS: *Open channel Junction, Schwarz-Christoffel Transformation, Dividing Flow*.

NOMENCLATOR

The following symbols are used in this paper:

a, b, c, d, j, f and h	Real unknown parameters depending on junction geometry	X_S	Relative flow depth
		Z_n	Complex position in physical plane $=x_n + iy_n$
B_S	width of the channel	ω	Complex potential $= \Phi + i\,\psi$
F_S	Froude number in a channel		
G	Acceleration of gravity	Ψ	Stream function
N	Complex constant	θ_1	first angle of intersection at the junction.
N	Subscript for Z-plane and λ – plane		
Q and Q_S	Flow rates in upstream main channel and in a tributary channel respectively.	θ_2	second angle of intersection at the junction.
		Φ	Velocity potential
U_S	Mean velocity in a channel	λ_n	Transformation plane $= \xi_n + i\,\eta_n$
W_S	Relative width of a channel	ω	Complex potential $= \Phi + i\,\psi$

Subscript s = in any of the quantities W_S, X_S, Q_S, U_S, Y_S, F_S and B_S when no sub-s is used, the symbol refers to the upstream main-channel
When s =1, the symbol refers to the main channel extension.
When s =2 or 3, the symbol refers to the branch of angle θ_1 or θ_2 respectively.

INTRODUCTION

For a specific dividing flow (T-junction), Taylor [1] carried out the first experiments on the problem. He suggested graphical representation in terms of discharges ratio and depths ratio. Neary and Odgaard [2] investigated the flow structure at 90° open channel diversion. From the velocity data, they [2] concluded that the flow at open channel diversion is a three-dimensional flow. Dividing flow in open channel junction generated theoretical interest due to a number of important flow phenomena involved. Detailed hydrodynamics of junction flow are found to be complex and there exist a number of parameters that characterizes the flow physics. This includes the size, shape, slope, angles between the dividing channels and the flow Reynolds and Froude numbers. Thereby, many investigators [1-13] studied this problem to stand on the main factors affecting this problem and determine the practical solutions. After investigating the flow at 90° open channel junction, Hsu [6] concluded that the energy heads upstream and downstream of the diversion almost be equal. After heir study on 90° open channel junction, Law and Reynolds [9] concluded that, at high Froude number (F>0.7) both the energy and momentum theories are inaccurate. Rashwan [11] developed a one-dimensional theoretical model for sub-critical flow in dividing open channel junction. He applied the momentum principles in the stream-wise direction to two control volumes in the junction. This allows the model to be easily implemented in network models [11].

The conformal mapping approach was first adopted for the problem of channel junctions with combining flow by Greated [5]. By using the Schwarz-Christoffel

transformation, he developed expression for locating the stagnation point for rectangular channel with 90° junction angle. Webber and Greated [12] began the focus on the general flow characteristics at an open-channel junction. Using conformal mapping, they were able to locate the stagnation point at the upstream corner of the channel junction and delineate the zone of separation. They also included a method for estimating the relative energy loss across the junction. Ali [3] applied the Schwarz-Christoffel transformation theory and the principle of conservation of energy to two-dimensional numerical model consists of main channel divided to one branch channel plus the extension of the main channel. Ali and Gommah [4] succeeded for the second time to apply the same previous technique plus super-position technique according to Milne-Thomson [15] to evaluate the flow characteristics at open channel junction. Hassenpflug [7] had derived equations of free-streamline flow of a branched channel in plane incompressible flow using the hodograph method combined with Blasius-Prandtl method. He [7] also gave correct results of Modi et al. [10] and Sinha and Odgaard. [14].

This research aims to investigate numerically and experimentally the influence of both the junction geometry and flow type in the main channel on the divided flow characteristics in the tributary channels.

SIMULATION OF THE NUMERICAL MODEL

***Assumption*:** Figure (1-a) shows the junction geometry considered as an extension of the main channel. The main assumptions in this analysis are: 1) The channel junction is in rectangular shape with horizontal smooth bed. 2) The flow is irrotational and subcritical. 3) The flow velocity in the branch channels is uniform irrespective of the reverse influence of the tributaries on the velocity distribution in the main extension. 4) The loss of energy in the short junction is negligible.

Theory: In order to obtain a general solution of the problem, the various boundaries of a channel junction, as represented in the Z-plane ($Z= x +iy$) as shown in Fig. (1-a) must be transformed to the real axis of a λ-plane ($\lambda= \xi + i\ \eta$) as shown in Fig. (1-b), the points within the region of flow between the boundaries are transformed to the corresponding points in the upper half of the λ-plane ($\lambda= \xi + i\ \eta$). By using the theorem of Schwarz-Christoffel, the corresponding expression for the transformation is as follows [15]:

$$dZ / d\lambda = N (\lambda-b)^{(\theta_2/\pi)} (\lambda-d)^{(1-\theta_2/\pi)} (\lambda-j)^{(1-\theta_1/\pi)} (\lambda-a)^{(-1)} (\lambda-f)^{(-1)} (\lambda-h)^{(-1)} (\lambda-c)^{(-1)} \quad \ldots\ldots\ldots \quad (1)$$

where N is a complex number, b, d, j, a, f, h and c are real unknown parameters determined from the geometric dimensions of the junction, and θ_1 and θ_2 are the junction angles.

Determination of Subsidiary Parameters: Schwarz-Christoffel transform-ation involves unknown parameters, which must be determined before the mapping, can be applied to the physical problem. All the previous works determined these parameters using various integration methods along the real axis of the λ plane, together with some form of iterative procedure. Some examples of such methods are presented in [3,4,7,10,15,16-18]. Milne-Thomson [15] gave analytic solution by using a hodograph

method, Modi et al. [10], Ali [3] and Ali and Gommah [4] have used conventional Schwarz-Christoffel transformation to map walls on a straight line. They obtained analytically the mapping of the corner points

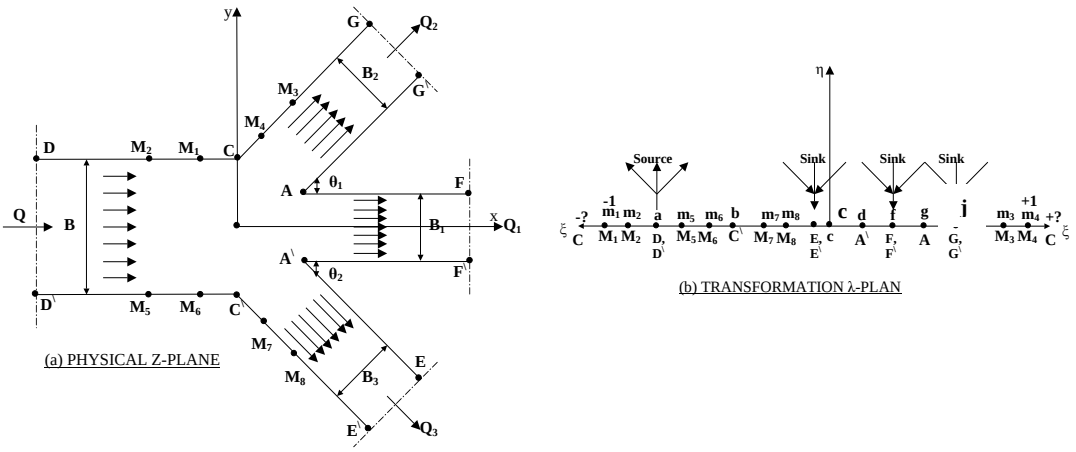

Fig. (1) Definition sketch Physical and Transformation planes

Chaung et al. [16] integrated along the real axis in the λ plane to determine the lengths of all sides, and applied Kantorovich and Krylov [19] method to evaluate the singular integrations by separating the improper integral into two parts, namely a finite form in a continuous region which can be integrated exactly and a definite integral which is free of any singularity. The Gauss-Jacobi quadrature was used to evaluate these integrals. The most used iterative procedure is the Newton-Raphson method, with the Jacobian matrix approximated by a finite difference quotient matrix, as applied to branched channels by Hassenpfug [7]. Trevelyan et al. [18] had used an alternative integration approach from that employed by Hassenpflug [7] in the iterative mathematical technique for determining the parameters involved in the Schwarz-Christoffel transformation

Numerical solutions are also available by using standard programs SCPACK by Trefethen [20], or Algorithm 756 of MATLAB by Driscoll [21] who compute points in the physical plane by numerical integration of the Schwarz-Christoffel integral. In this research, the Algorithm 756 of MATLAB by Driscoll [21] is used to find the unknown parameters.

Discharge and Flow Depth: In the transformation plan (λ-plane), if a source at point D (Fig.1-a) of strength (UB/π) and three sinks at points F, G and E of strength (U_1B_1/π), (U_2B_2/π) and (U_3B_3/π) respectively, the complex potential in (λ-plane) may be given by:

$$\omega = (- UB*\ln(\lambda-a))/\pi + (U_1B_1*\ln(\lambda-f))/\pi + (U_2B_2*\ln(\lambda-h))/\pi + (U_3B_3*\ln(\lambda- c))/\pi \quad (2)$$

$$d\omega/d\lambda = (-UB/(\pi(\lambda-a)) + (U_1B_1/\pi(\lambda-f)) + (U_2B_2/\pi(\lambda-h)) + (U_3B_3/\pi(\lambda-c) \quad (3)$$

$$d\omega/dZ = d\omega / d\lambda * d\lambda / dz \quad (4)$$

With the substitution from Eqns. (1 and 3) into Eqn. (4) that is:

$$d\omega/dz = (-UB(\lambda-c)(\lambda-f)(\lambda-h) + U_1B_1(\lambda-a)(\lambda-c)(\lambda-h) + U_2B_2(\lambda-a)(\lambda-c)(\lambda-f) + U_3B_3(\lambda-a)(\lambda-f)(\lambda-h)) * (1/(\pi N(\lambda-b)^{(\theta_2/\pi)} (\lambda-d)^{(1-\theta_2/\pi)} (\lambda-j)^{(1-\theta_1/\pi)})) \ldots\ldots\ldots \quad (5)$$

At the stagnation points A and A' in Fig. (1)

$d\omega/dz=0$, $\lambda=$ j and $d\omega/dz=0$, $\lambda=$d respectively, so Eqn. (5) becomes:

$(-UB/(j-a)) + (U_1B_1/(j-f)) + (U_2B_2/(j-h)) + (U_3B_3/(j-c)) = 0.$ …… (6)

$(-UB/(d-a)) + (U_1B_1/(d-f)) + (U_2B_2/(d-h)) + (U_3B_3/(d-c)) = 0.$ …… (7)

For dimensionless form let us consider:

K= Relative velocity. $K_1= U_1/U$, $K_2= U_2/U$ and $K_3= U_3/U$

W= relative width. $W_1= B_1/B$, $W_2= B_2/B$ and $W_3= B_3/B$

So Eqns. (6 and 7) may be re- written as:

$(K_1W_1/(j-f)) + (K_2W_2/(j-h)) + (K_3W_3/(j-c)) + (-1/(j-a)) = 0.$ …… (8)

$K_2 = ((1/(j-a)) – (K_1W_1/(j-f)) – (K_3W_3/(j-c)))* ((j-h) / W_2).$ … …… (9)

$(K_1W_1/(d-f)) + (K_2W_2/(d-h)) + (K_3W_3/(d-c)) + (-1/(d-a)) = 0.$ …… (10)

$K_3 = ((1/(d-a)) – (K_1W_1/(d-f)) – (K_2W_2/(d-h)))*((d-c) / W_3).$ …… …… (11)

By the substitution from Eqn. (11) into Eqn. (8), one has;

$K_2W_2((1/(j-h)) – ((d-c)/((d-h)*(j-c)))) + K_1W_1 ((1/(j-f)) – ((d-c)/((j-c)*(d-f)))) – ((1/(j-a)) – ((d-c)/((d-a)*(j-c)))) = 0.$ …… (12)

$K_2W_2C_1 + K_1W_1C_2 – C_3 = 0$ …… (13)

$K_2 = (C_3 – K_1W_1C_2)/ (W_2C_1)$ …… (14)

where;

$C_1 = ((1/(j-h)) – ((d-c)/((d-h)*(j-c))))$

$C_2 = ((1/(j-f)) – ((d-c)/((j-c)*(d- f))))$

$C_3 = ((1/(j-a)) – ((d-c)/((d-a)*(j-c))))$ …… (15)

Substitution from Eqn. (9) into Eqn. (10), it yields

$K_1W_1 ((1/(d-f))- ((j-h)/((j-a)*(d-h)))) + K_3W_3 ((1/(d-c))- ((j-h)/((j-c)*(d-h)))) – ((1/(d-a))- ((j-h)/((j-a)*(d-h)))) = 0$ …… (16)

$K_1W_1C_4 + K_3W_3C_5 – C_6 = 0.$ …… (17)

$K_3 = (C_6 – K_1W_1C_4) / (W_3C_5).$ …… (18)

Where;

$C_4 = ((1/(d-f))- ((j-h)/((j-a)*(d-h))))$

$C_5 =((1/(d-c))- ((j-h)/((j-c)*(d-h))))$

$C_6 = ((1/(d-a))- ((j-h)/((j-a)*(d-h))))$ …… (19)

In this simulation, the flow in the junction is assumed to be subcritical flow ($F \leq 0.7$) and the energy loss due to the formation of eddies or the flow deflection or both is disregarded. Therefore, the application of energy conservation in the main and the diverging branches gives:

$Y + U^2/2g = Y_1 + U_1^2/2g$ …… (20)

$Y + U^2/2g = Y_2 + U_2^2/2g$ …… (21)

$Y + U^2/2g = Y_3 + U_3^2/2g$ …… (22)

In the dimensionless form, Eqns. (20, 21 and 22) may be rearranged as:

$X_1 = 1+ 0.5 F^2 (1- K_1^2)$ …….. (23)
$X_2 = 1+ 0.5 F^2 (1- K_2^2)$ …….. (24)
$X_3 = 1+ 0.5 F^2 (1- K_3^2)$ …….. (25)
$Q = Q_1 + Q_2 + Q_3$ …….. (26)
$UBY = U_1B_1Y_1 + U_2B_2Y_2 + U_3B_3Y_3$ …….. (27)

In dimensionless form Eqn. (27) becomes;

$K_1W_1X_1 + K_2W_2X_2 + K_3W_3X_3 = 1$ …….. (28)

By substitution from Eqns. (14, 18, 23, 24 and 25) into Eqn. (28) one have;

$K_1W_1(1+0.5F^2 (1-K_1^2)) + ((C_3 – K_1W_1C_2)/C_1)*(1-0.5F^2$
$(1-((C_3-K_1W_1C_2)/W_2C_1)^2)) + ((C_6 – K_1W_1C_4)/C_5)*$
$(1-(1+0.5F^2 (1- ((C_6 – K_1W_1C_4)/W_3C_5)^2)) = 1$ …….. (29)

For the known values of F, W_1, W_2 and W_3, Eqn. (29) is solved by MATLAB function for finding the roots to determine the values of K_1. Thereafter, the values of K_2, K_3 are obtained from Eqns.(14) and (18) respectively. Then the relative depths X_1, X_2 and X_3 are found from Eqns. (23, 24 and 25).

Computer Facility: Flow chart of the main program***;* A MATLAB Version 6.0.0.88*** program was written for digital computer. Shown in Fig (2) is the flow chart, which explains, the essential features of this program.

Range of variable parameters: Intersection angles θ_1 and θ_2 varied to take 90°, 60° and 30° for each, relative widths of the branched channels W_1, W_2 and W_3 varied from1 to 0.3 with step 0.1 for each and Froude number in the main channel, F varies from 0.0 to 0.7 with step 0.1.

Input data*:* Intersection angles θ_1 and θ_2, relative widths of the branched channels W_1, W_2, and W_3. and Froude number in the main channel, F.

Output data*:* The following outputs may be taken from the program: Froude numbers in tributary channels, F_1, F_2 and F_3. The relative flow depths Y_1/Y, Y_2/Y and Y_3/Y. The relative flow rates Q_1/Q, Q_2/Q and Q_3/Q.

EXPERIMENTAL WORK AND PROCEDURE

The experimental tests were executed in small, horizontal, rectangular channels. The channels were made of wood. The main channel and its extension have constant width of 200 mm and total length of 4.00 m. The widths of the branches were changed to take 100, 150 and 200 mm while their lengths were constant at 2.00 m. The intersection of the branches with the main channel was located at 2.00 m from its entrance.

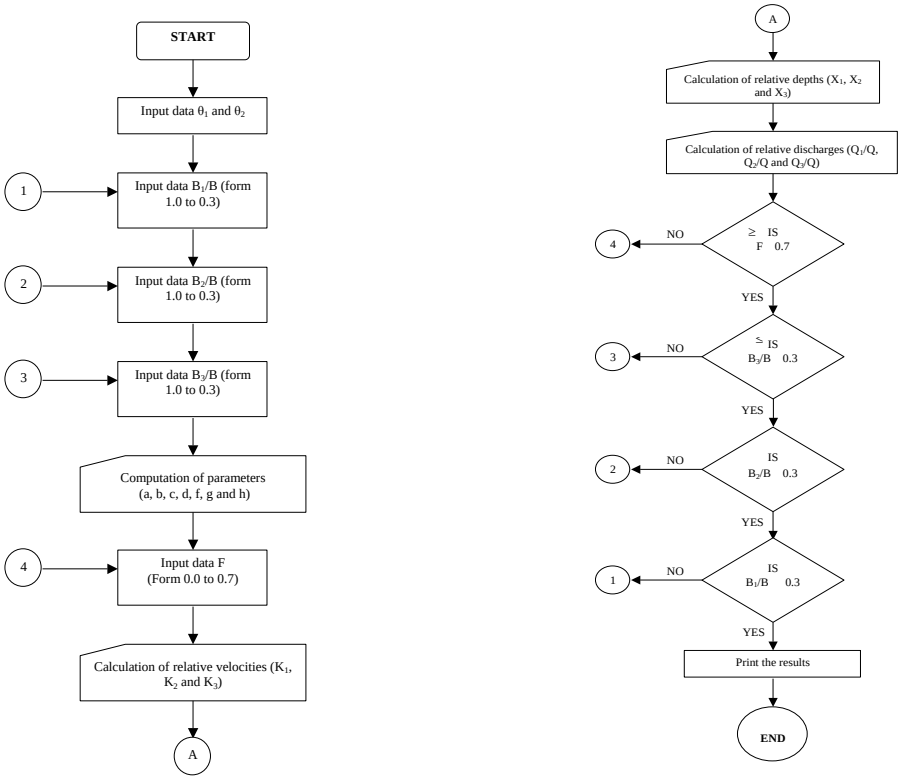

Fig (2) Flow chart of the computer program

Figure (3) gives a general view of the experimental setup. The intersection angles were varied to take 90°, 60° and 30° for each. Water depths in branched channels were controlled to be same as in the numerical model by means of vertical gates located at the end of each and were measured using point gauges. To avoid the backwater effect and flow disturbances, the mean depth of each channel was taken at a station 1.2 m from the center of the junction [2]. The inflow rates were regulated by a gate valve and were measured by a calibrated flow meter. The branched channels flow rates were measured volumetrically. The total inlet flow rates were ranged from 3.0 liters/sec to 15 liters/sec.

Model Verification: A series of laboratory tests was performed on the dividing flow at horizontal channel junction having three tributary branches for different junction angles and different relative branches bed width. Water depths in the experiments were taken to be same as in the numerical model and the corresponding discharges were measured. Figure (4) shows the plotting of the experimental mean relative discharge values $(Q_1/Q)_{meas}$, $(Q_2/Q)_{meas}$ and $(Q_3/Q)_{meas}$. versus the mean relative discharge values $(Q_1/Q)_{num}$, $(Q_2/Q)_{num.}$ and $(Q_3/Q)_{num.}$ predicted from the numerical solution. A well agreement between the experimental and the numerical results is noticeable, especially for low discharges. The deviation between the results at high

discharges may due to the formation of high turbulence at the junction in the experiments produces energy losses, while these losses of energy are neglected in numerical solution.

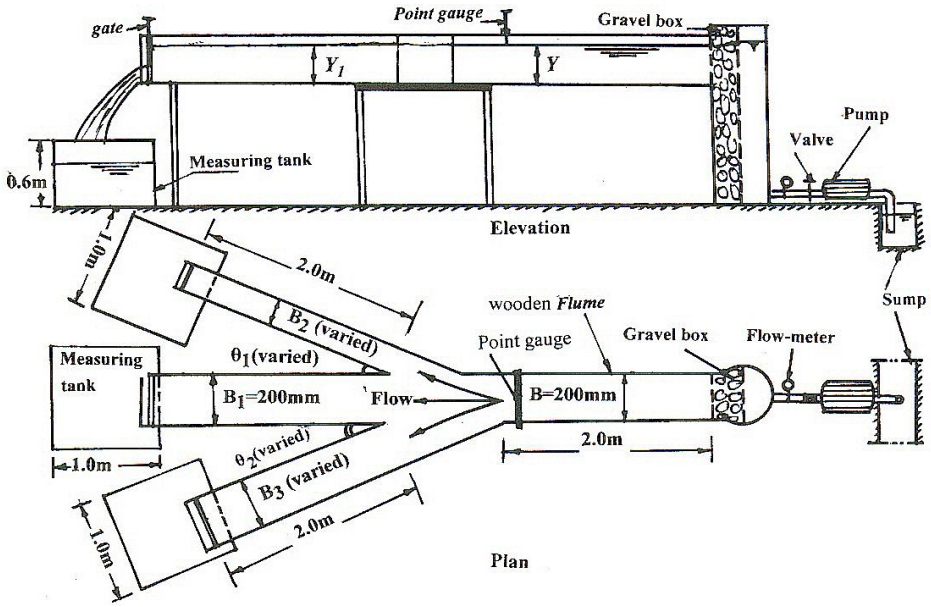

Fig. (3) Experimental setup.

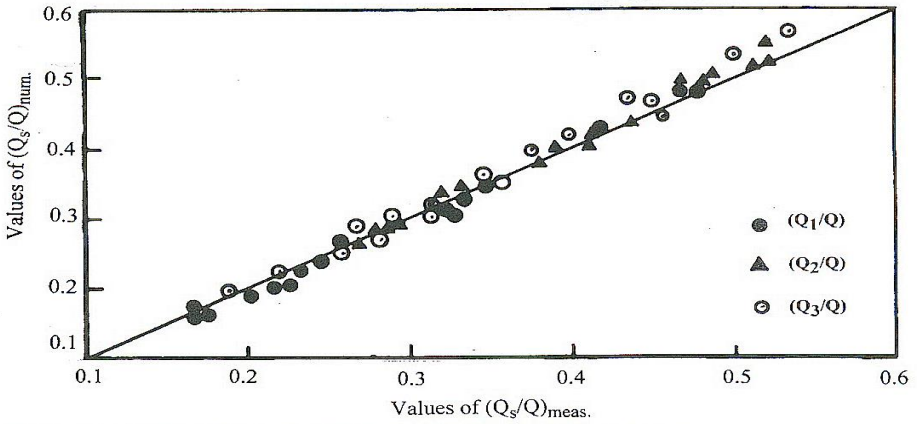

Fig. (4) Numerical results of the mean relative discharges $(Q_S/Q)_{num}$ versus the experimental ones $(Q_S/Q)_{meas}$. (s =1,2,3)

ANALYSIS OF THE NUMERICAL RESULTS AND DISCUSSIONS

***Relative Discharge in The Tributary Channels*:** The values of Froude number in the main channel, F were drawn versus the relative discharge in branch channels Q_1/Q and Q_3/Q for different junction angles and relative widths of the branch channels. An

example is shown in Fig. (5). It is obviously that the discharge in the branch channels is independent of the main channel Froude number.

Figures (6 and 7) show the variation of mean relative discharge Q_1/Q and Q_3/Q with the relative width B_3/B and B_2/B as a third variable at $B_1/B=1.0$, $\theta_1=90°$ and $\theta_2=90°$ and 30° respectively The relative discharge Q_3/Q increases with the increase of ratio B_3/B, consequently Q_1/Q values are decreasing by different percent according to B_2/B ratios. For constant value of θ_1 and B_1/B, the decrease of θ_2 from 90° to 30° decreases the discharge ratio Q_3/Q by about 29.5% and increases the relative discharge ratio Q_1/Q by about 20%. Also, the relative discharge ratio Q_2/Q in the second branch of width B_2 is obtained from the continuity equation as: $Q_2/Q = 1 - (Q_1/Q + Q_3/Q)$.

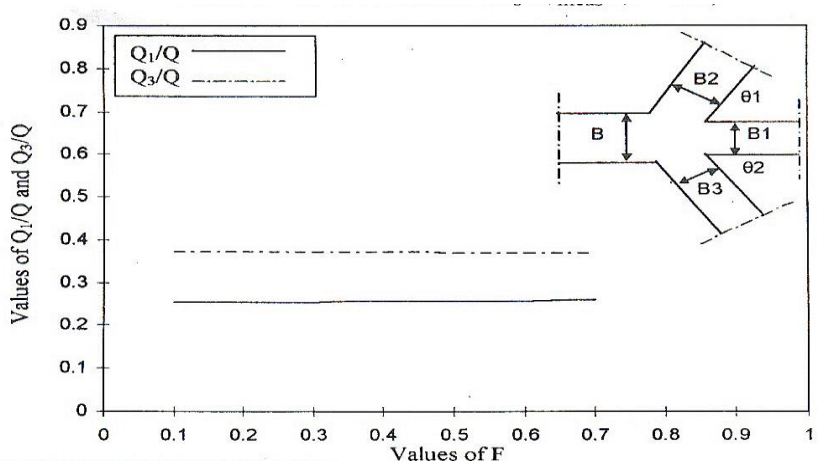

Fig. 5 Variation of Q_1/Q and Q_3/Q versus F at
($B_1/B=B_2/B=B_3/B=1$ and $\theta_1=\theta_2=60^o$)

To study the effect of varying the ratio B_1/B on the dividing discharges at the junction, the values of θ_1 and θ_2 are kept constants at 60° and the numerical results of B_3/B and both Q_1/Q and Q_3/Q are plotted in Figs. (8 to 10). The values of B_2/B are changed to take values between 0.3 and 1.0 and plotted as a third dimension in all the figures. The same trend of the results is seen, where the values of Q_1/Q decrease with increasing of B_3/B.

For constant value of B_3/B the increase of B_2/B decreases the values of Q_1/Q. It is noticed from Figures that the rate of decreasing Q_1/Q with the change B_2/B is decreased with the decrease of B_1/B till it becomes unreliable or ineffective on Q_1/Q when B_1/B is equal or less than 0.4 Also, from these Figures, it is noticeable that the decrease of relative width B_1/B from 1.0 to 0.3 decreases the relative discharge Q_1/Q by 79% and increases Q_3/Q by 78%, and the effect of B_3/B on Q_3/Q decrease with the decrease of B_1/B. For the influence of B_2/B on both relative discharges Q_1/Q and Q_3/Q, the results show that the decreasing of B_2/B from 1.0 to 0.3 increases Q_1/Q by 87% and Q_3/Q by 22%. Also, the increase of the relative width B_3/B from 0.3 to 1.0 decreases Q_1/Q by 48% and increases Q_3/Q by about 22%.

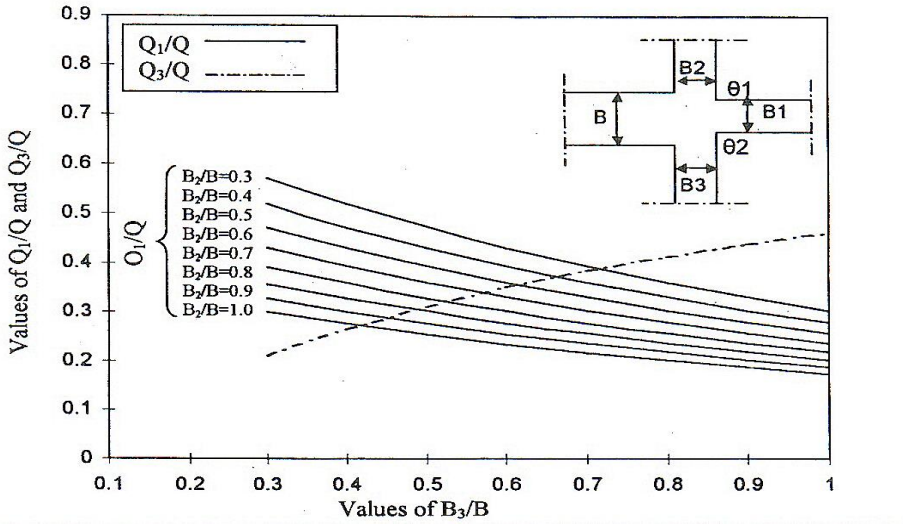

Fig. 6 Variation of Q_1/Q and Q_3/Q versus B_3/B for various values of B_2/B at ($B_1/B=1$ and $\theta_1=\theta_2=90^o$)

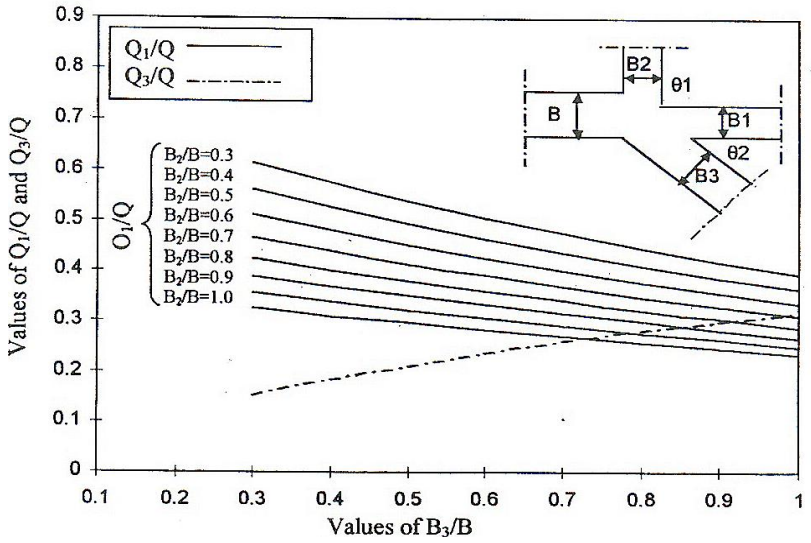

Fig. 7 Variation of Q_1/Q and Q_3/Q versus B_3/B for various values of B_2/B at ($B_1/B=1$ and $\theta_1=90^o$ and $\theta_2=30^o$)

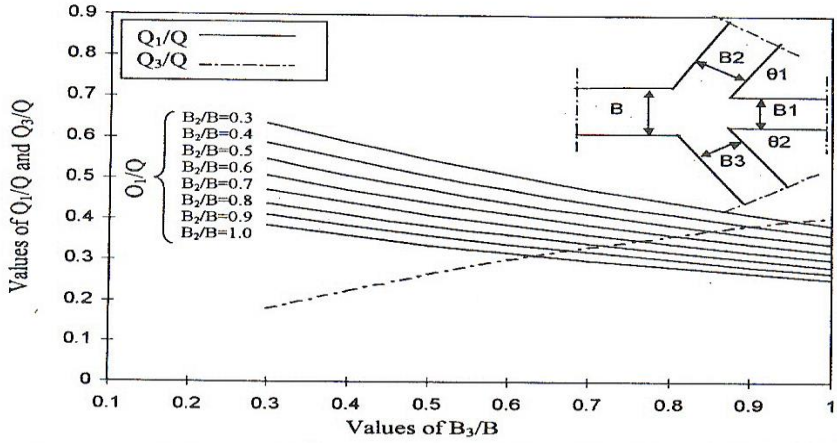

Fig. 8 Variation of Q_1/Q and Q_3/Q versus B_3/B for various values of B_2/B at (B_1/B=1 and $\theta_1 = \theta_2 = 60^o$)

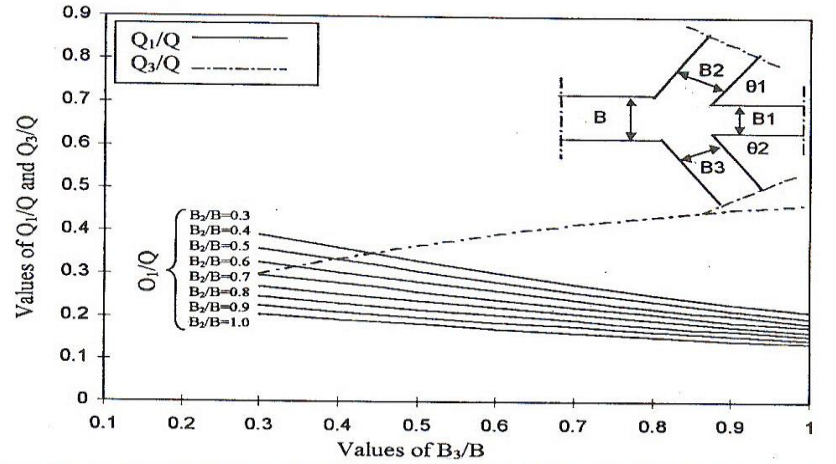

Fig. 9 Variation of Q_1/Q and Q_3/Q versus B_3/B for various values of B_2/B at (B_1/B=0.6 and $\theta_1 = \theta_2 = 60^o$)

Froude Numbers in The Tributary Channels: Froude number may represent the flow characteristics either in the main channel extension or in the tributary channels. The numerical results (as example) are plotted in Figs. (11 and 14) to illustrate the variation of Froude numbers in the tributary channels (F_1, F_2, and F_3) with Froude number in the main channel (F) for various values of θ_1 and θ_2, at a range of B_3/B from 0.3 to 1.0 with different values of B_1/B and B_2/B. Values of Froude number in the tributary channels (F_1, F_2 and F_3) increase with the increase of the value of Froude number in the main channel F. F_1 and F_3 are dependent on the width ratio B_3/B while the values of F_2 is independent of the width ratio B_3/B. The rate of increasing F_3 with decreasing B_3/B decreases with the decrease of θ_2, while F_1 values are decreased with the decrease of θ_1.

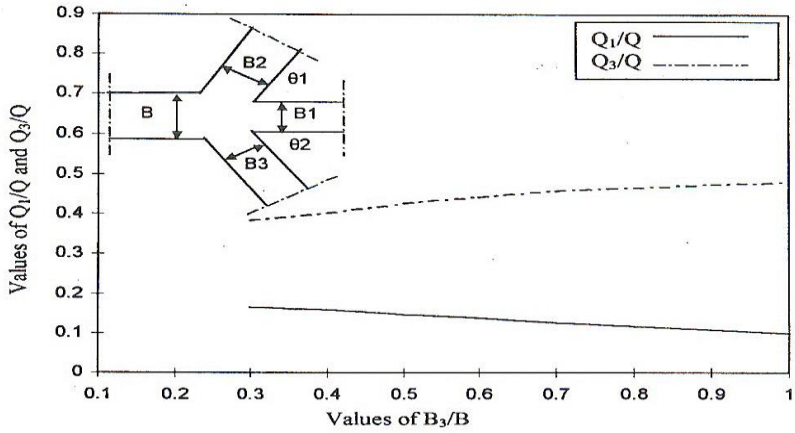

Fig. 10: Variation of Q_1/Q and Q_3/Q versus B_3/B for various values of B_2/B at (B_1/B=0.4 and $\theta_1 = \theta_2 = 60^o$)

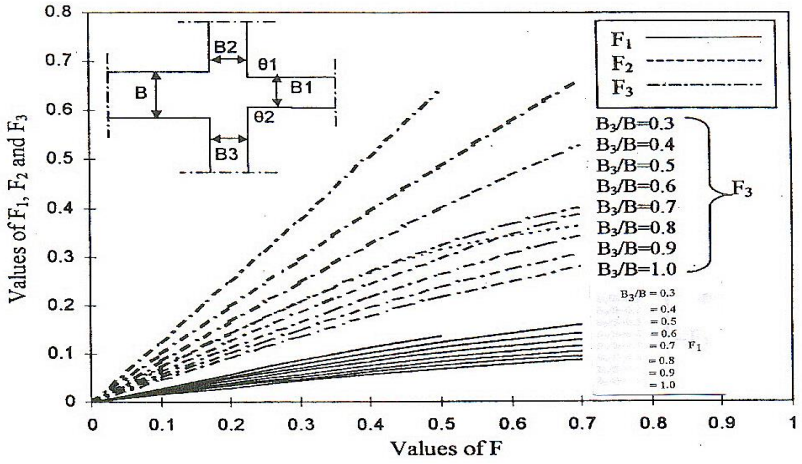

Fig. 11 Variation of F_1, F_2 and F_3 versus F for different values of B_3/B at ($B_1/B = B_2/B$ = 0.6 and $\theta_1 = \theta_2 = 90^o$)

The relations show also, that the rate of the increase of F_3 with B_3/B decreases with the decrease of θ_2 values. Also these figures indicate that, for constant values of θ_1, B_1/B and B_2/B the rate of increasing, F_1 with F is increasing but the rate of increasing F_3 with F is decreasing. For example when θ_2=90°, F_1 varies from 0.0171 to 0.0192 while for θ_2=30°, F_1 varies from 0.0227 to 0.125. Also, for θ_2=90°, F_3 varies from 0.04 to 0.2139 while for θ_2=30°, F_3 varies from 0.0246 to 0.1364.

The relative width B_1/B of the main channel extension is an important parameter for defining the state of flow in the tributary channels. The following example illustrates this fact quite well. When θ_1=90°, θ_2=30°, B_2/B and B_3/B=1.0 and F varies in range from 0.1 to 0.7, at B_1/B=1.0, F_1 varies from 0.0241 to 0.1324, while at B_1/B=0.6, F_1 varies from 0.0126 to 0.0716. So, the influence of relative width B_1/B on the Froude number in the extension of the main channel F_1 is noticed, where by decreasing B_1/B from 1.0 to 0.6, F_1 decreases by about 50%. Also, in these Figures, the

influence of the relative width of the extension of the main channel B_1/B on Froude number of the second branch channel F_2 is clearly shown, while F_2 is shown independent of the values of B_3/B. The rate of increasing F_2 with B_1/B is constant.

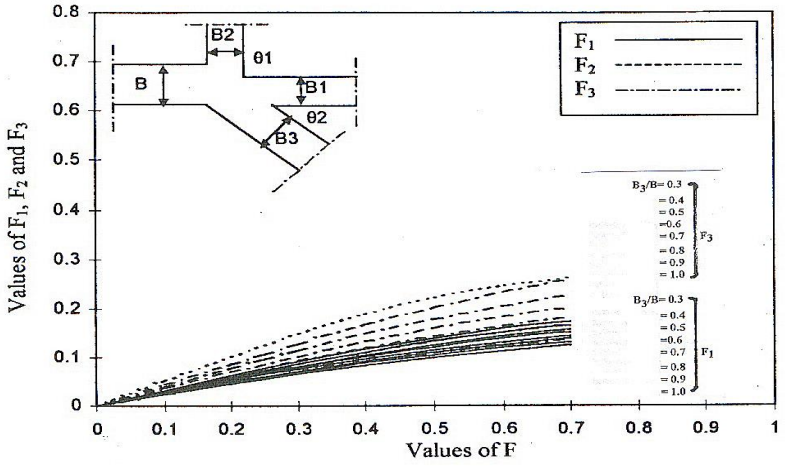

Fig. 12 Variation of F_1, F_2 and F_3 versus F for different values of B_3/B at (B_1/B= B_2/B = 1.0 and θ_1=90^o θ_2=30^o)

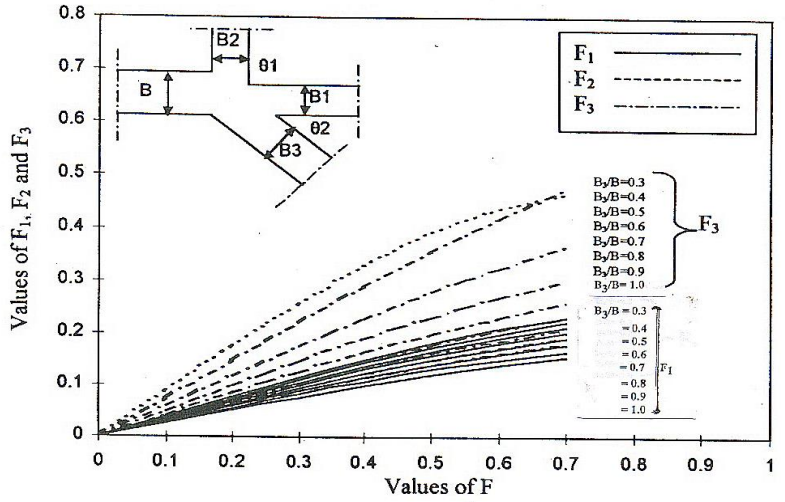

Fig. 13 Variation of F_1, F_2 and F_3 versus F for different values of B_3/B at (B_1/B= B_2/B = 0.6 and θ_1=90^o θ_2=30^o)

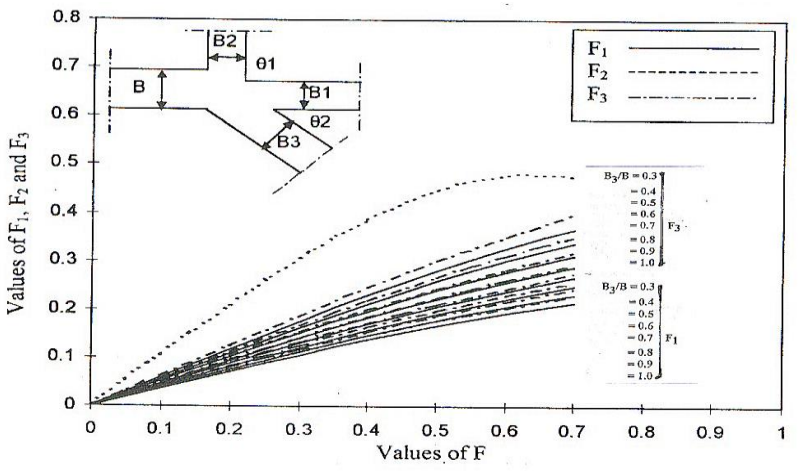

Fig. 14 Variation of F_1, F_2 and F_3 versus F for different values of B_3/B at (B_1/B=0.6, B_2/B = 0.3 and θ_1=90^o θ_2=30^o)

The influence of the relative width of the main channel extension B_1/B on F_3 is the same as F_2 where by decreasing B_1/B form 1.0 to 0.3, (F_2) values increases by about 47%. As we mentioned above that the relative width of the extension of the main channel B_1/B has the same as F_2 and F_3, while the decreasing of B_1/B from 1.0 to 0.3, F_3 increases by about 10%. The width of the second branch channel B_2/B is an important parameter that may define the state of flow of subcritical, critical or supercritical in the tributary channels. The comparison of data shown in Figs. (11 to 14) where B_2/B changes from 1.0 to 0.3 illustrate this fact very well. Where by decreasing B_2/B, the values of F_1 are increasing. This can be verified as follows, when θ_1=90°, θ_2=30°, B_1/B=0.6, B_3/B=0.7 and F varies in range from 0.1 to 0.7 for B_2/B=1.0, F_1 varies from 0.0249 to 0.1380, while for B_2/B=0.3 F_1 varies from 0.0447 to 0.2674. So, by decreasing the relative width of the second branch B_2/B from 1.0 to 0.3 Froude number in the extension of the main channel F_1 increases by about 85%. Also, it is seen that, F_2 increases by about 75% by decreasing B_2/B from 1.0 to 0.3, while F_3 increases by about 48% for the same trend of decreasing of B_2/B.

Relative depths in The Tributary Channels: The numerical results of the relative depth in the main channel extension (Y_1/Y), and in the tributary channels (Y_2/Y and Y_3/Y) versus Froude number in the main channel, F are plotted in Figs. (15 to 17). The relative flow depths (Y_1/Y, Y_2/Y and Y_3/Y) increase with the increase of Froude number in the main channel. The increase of the Froude number in the main channel, F from 0.0 to 0.7, the relative flow depths in the tributary channels (Y_1/Y, Y_2/Y and Y_3/Y), increase by about 22%. So, the main channel Froude number (F) is considered very important parameter affecting the relative depths in the tributary channels (Y_1/Y, Y_2/Y and Y_3/Y).

The influence of the angles of intersection at the junction (θ_1 and θ_2) on the relative depths in tributary channels (Y_1/Y, Y_2/Y and Y_3/Y) is also shown in Figures. From these Figures, it is clearly seen that the relative depth ratios independent on both θ_1 and θ_2, where the maximum difference in the calculated values of the tributary

channels Y_1/Y, Y_2/Y and Y_3/Y with the variation of θ_1 and θ_2 from 90˚ to 30˚ is not exceeding 3%. The variation of the relative widths of the tributary channels (B_1/B, B_2/B and B_2/B) with the relative depths (Y_1/Y, Y_2/Y and Y_3/Y) for θ_1=90°, θ_2=30° are shown also in Figs. (15 to 17). The relative flow depths in the tributary channels have slightly changes. So we can say that the relative depth ratios (Y_1/Y, Y_2/Y and Y_3/Y) are independent on the relative width ratios (B_1/B, B_2/B and B_3/B).

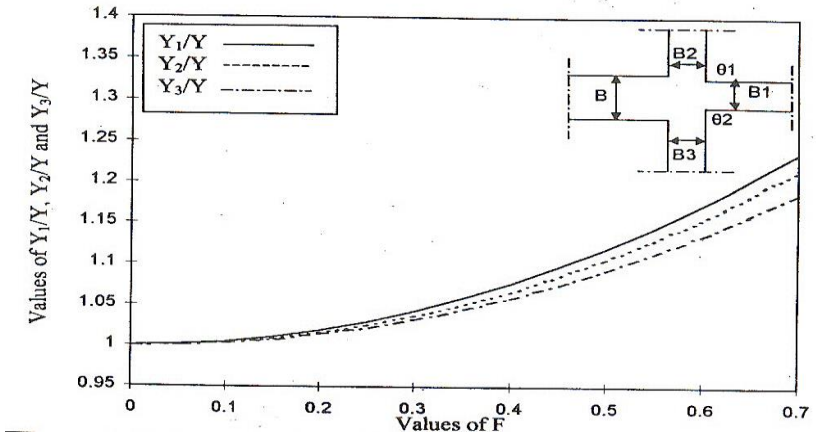

Fig. 15 Variation of Y_1/Y, Y_2/Y and Y_3/Y versus F for (B_1/B= B_2/B = 1.0 and θ_1= θ_2=90^o)

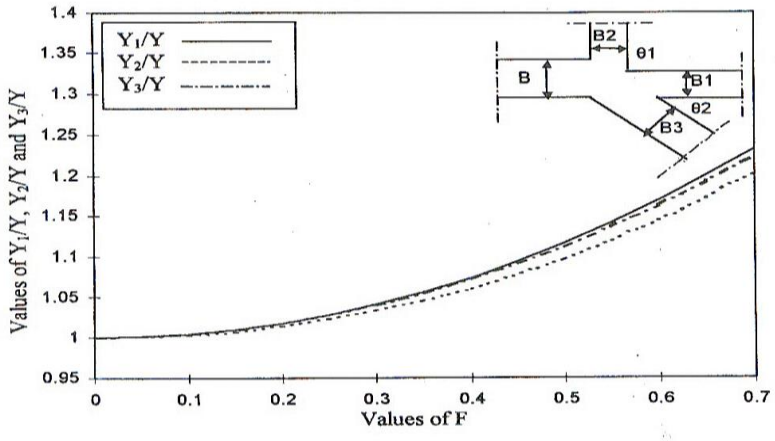

Fig. 16 Variation of Y_1/Y, Y_2/Y and Y_3/Y versus F for (B_1/B= B_2/B = 1.0, θ_1= 90^o and θ_2=30^o)

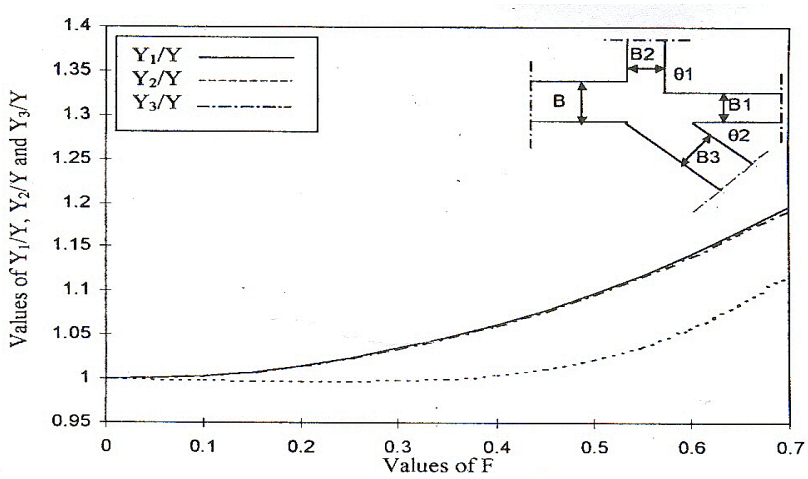

Fig. 17 Variation of Y_1/Y, Y_2/Y and Y_3/Y versus F for (B_1/B=0.8, B_2/B =0.3, θ_1= 90^o and θ_2=30^o)

CONCLUSIONS

A numerical solution for the problem of dividing flow at open channel junction has been obtained. Such a numerical model presents quantitative conclusion, which could be helpful in developing insight about flow behavior at open channel junction. From the presented model and for sub-critical flow in main channel, the following conclusions may be drawn:

1- The flow rates either in the main channel extension or in the branch channels depend largely on the geometric dimensions of the junction [angles of intersection at the junction (θ_1 and θ_2) and relative width of tributary channels].
2- Froude number in main channel has negligible influence on flow rates in the branches.
3- The flow characteristic in the main channel extension as well as in the branched channels are dependent on the flow behavior in the main channel (represented by Froude number, F) and the geometric dimensions of the junction [angles of intersection at the junction (θ_1 and θ_2) and relative width of tributary channels].
4- The relative flow depths in the tributary channels (Y_1/Y, Y_2/Y and Y_3/Y) depend on the flow characteristic of the flow in the main channel represented by Froude number and independent of the junction geometry.

REFERENCES

1- Taylor, E.H., "Flow characteristics at rectangular open channel junction", Trans., ASCE, Vol. 109 pp. 893- 902, Nov. 1944.
2- Neary, V.S., and Odgaard, J.A.," Three dimensional flow at open channel diversion", J. Hydr. Eng., ASCE, 119(11), Nov.1993.
3- Ali, N. A., "A theoretical study of dividing flow in an open channel junction", Bulletin of the Faculty of Eng., Assiut University Vol. 18, No. 2, 1990.

4- Ali, N.A. and Gommah, E.E.,"Numerical analysis of potential flow segmentation at open channel diversion", Bulletin of the Faculty of Eng., Assiut University, 24 (2), 1996.
5- Greated, C. A., "A theoretical study of flow behavior at open channel junctions". Researches report No.6, University of Southampton, Department of Civil Engineering, England, Feb. 1964. (Cited from Ref. 13).
6- Hus, C.C, Wu, F.S, and Lee,W.J.," Flow at 90^{o} equal-width open channel junction", J. Hydr. Eng., ASCE, 124(2), pp. 186-191, Feb.1998.
7- Hassenpflug, W. C., "Branched channel free-streamlines", Comput. Meth. Appl. Mech. Engrg. 159 (3/4), pp.329-354, 1998.
8- Larry, J. W., Schumate, E. D.,and Mawer. N., " Experiments on flow at a 90° open-channel junction". Jour. of Hydr. Eng., ASCE, 127 (5), pp. 340-350, May 2001.
9- Law, S. W. and Reynolds, A. J., " Dividing flow in an open channel", Jour. of Hyd. Div., ASCE, Vol., 92,No. HY3, pp. 207-230, 1966.
10- Modi, P. N., Ariel, P. D., and Dandekar, M. M. "Conformal mapping for channel junction flow", Jour. Of Hyd. Div., ASCE, Vol. 107, No. HY12, Dec. 1981.
11- Rashwan, I.M.H.," Dynamic model for sub-critical dividing flow in open channel junction",Proc. Of 8^{th} Int. Water Tech. Conf.,IWTC, 2004, Alexandria, Egypt.
12- Webber, N. B., and Greated, C. A. "An investigation of flow behavior at the junction of rectangular channels." Proc., Instn. Of Civ. Engrs., Vol.34, Thomas Telford Ltd., London, pp. 321-334, 1966 (Cited from Ref. 8).
13- Yoshimi, Y. A. and Stelson, T. E., "Grit unbalance in sewage flow division", Jour. of sanitary Eng. Div., ASCE, Vol. 89, SA2, pp. 61- 82, 1953.
14- Sinha, S. K., and Odgaard, A. J., "Application of conformal mapping to diverging open channel flows". Jour. of Engrg. Math. 30, pp. 355-363, 1996. (Cited from Ref. 7).
15- Milne-Thomson, "Theoretical Hydrodynamics", 5^{th} Edition, Macmillan Press, 1979.
16- Chaung, J. M., Gui, Q. Y., and Hsiung, C. C., "Numerical computation of Schwarz- Christoffel transformation for simply connected unbounded domain", Comput. Meth. Appl. Mech. Engrg. 105, pp.93-109, 1993. (Cited from Ref. 18).
17- Gribnyak, S. T., Logvinenko, A. V., Romanenko, V. N., Fedorovich, A. Y., and Ennan, A. A., "Numerical investigation of the 2-dimensional potential flow of an ideal fluid using the Schwarz-Christoffel integral", Compt. Maths. Phys. 31 (8), pp.74-79, 1991. (Cited from Ref. 18)
18- Trevelyan, P. M. J., Illiot, L., and Ingham, D. B., "Potential flow in a finite channel with multiple sub-channels using the Schwarz-Christoffel transformation", Comp. Meth. Appl. Engrg. 189, pp. 341-359, 2000.
19- Kantorovich, L. V., and Krylov, V. I., "Approximate Methods of Higher Analysis", Interscience, Noordhoff, pp. 521-542, 1958. (Cited from Ref. 18).
20- Trefethen, L. N., "Numerical computation of the Schwarz- Christoffel transformation", SIAM J. Sci. Stat. Comput. 1 (1), pp. 82-102, 1980. (Cited from Ref. 18).
21- Driscoll, T. A., "Algorithm 756: A MATLAB toolbox for Schwarz- Christoffel mapping", ACM Trans. Math. Softw. 22 (2), pp.168-186, 1996.

التحليل الرياضي و المعملي لتقسيم السريان في تفريعات القنوات المكشوفة ذات المدى القصير

تعتبر ظاهرة توزيع السريان في تفريعات القنوات المكشوفة ذات المدى القصير من الظواهر الهيدروليكية التى تستحق الاهتمام والدراسة، هذا التقسيم في السريان يحدث في مواقف عدة مثل تخطيط وتصميم قنوات الري كالترع والمصارف عندما تتفرع الترع الأعلى درجة الى عدد من الترع ذات الدرجة الأقل فى نقطة واحدة، أو كما يحدث في شبكات الصرف الصحي وداخل محطات معالجة مياه الصرف الصحي حيث تتفرع قناة المدخل الى عدد من القنوات الفرعية حسب أحواض المعالجة. كما أن تقسيم السريان يعتبر من الأعمال الرئيسية والظواهر المهمة في أعمال ومنشآت التحكم في مياه الري.

يقدم هذا البحث دراسة تحليلية رياضية ومعملية لتفرع السريان ذاتيا داخل القنوات المكشوفة اعتمادا على خصائص السريان في القناة الرئيسية (ممثلا برقم فرويد) وعلى الأبعاد الهندسية للتفريعة (ممثلا في النسبة بين عرض كل فرع إلى عرض القناة الرئيسية، وكذلك زاوية ميل كل فرع). باستخدام نظرية التوافق التصويري (نظرية شوارتز كريستوفيل)، ومبدأ الحفاظ على الطاقة (نظرية برنولى) تم الوصول إلى نموذج رياضي يحتوى على مجموعة من المعادلات الرياضية الغير خطية ممثلة لتفرع السريان المنتظم إلى ثلاث شعب فرعية. صيغت المعادلات الرياضية في صورة غير بعدية لتعميم النتائج وتم برمجة النموذج الرياضي على الحاسب الآلي لإمكانية حله. وبمعلومية معدل التصرف وعمق المياه ونوع السريان في القناة الرئيسية، وكذلك الأبعاد الهندسية للتفريعة، أمكن تقديرمعدل التصرف وعمق المياه ونوع السريان في كل فرع على حدة. تم تغيير رقم فرويد بالقناة الرئيسية في المدى من 0.1 إلى 0.7 ونسبة عرض آي فرع إلى عرض القناة الرئيسية في المدى من 0.3 إلى 1.0 وكذلك تم تغيير زاوية ميل كل فرع لتأخذ القيم 30، 60، 90 درجة. وللتحقيق من نتائج الحل الرياضي، تم عمل برنامج عملي معملي على قناة رئيسية بطول كلى 4.00 متر وبعرض 200 مم، وضعت التفريعة على بعد 2.00 متر من مدخلها وكان طول كل فرعه 2.00متر. تم تغيير عروض هذه التفريعات لتأخذ 100، 150، 200 مم، وكذلك زاوية ميل كل فرع على اتجاه السريان بالقناة الرئيسية لتأخذ 30، 60، 90 درجة لكل على حدة. بمقارنة النتائج المعملية بنظيراتها الرياضية لنسب معدلات التصرف بالتفريعات إلى معدل التصرف بالقناة الرئيسية، أمكن التحقق من دقة نتائج الحل الرياضي التي كان من أهمها: أنه لا توجد علاقة بين نسب تقسيم التصرف بين القنوات الفرعية الثلاثة ونوع السريان في القناة الرئيسية. أيضا أن نسب تقسيم السريان بين القنوات الفرعية الثلاثة تتوقف بشكل كبير على قيمتي زاويتي التفريعة وكذلك على نسبة عروض القنوات الفرعية إلى عرض القناة الرئيسية. كما أوضح النموذج أن نوع السريان في القنوات الفرعية الثلاث ممثلا في رقم فرويد يتوقف بدرجة كبيرة على نوع السريان بالقناة الرئيسية، كما يتوقف على الشكل الهندسي للتفريعة، وأن العمق النسبي للسريان بالقنوات الفرعية الثلاث لا يعتمد على الشكل الهندسي للتفريعة.